Method for fitting crystal field parameters and the energy level fitting for Yb^{3+} in crystal Sc_2O_3*

Zhang Qing-Li(张庆礼)[a)b)†], Ning Kai-Jie(宁凯杰)[a)], Xiao Jin(肖 进)[a)],
Ding Li-Hua(丁丽华)[a)], Zhou Wen-Long(周文龙)[a)], Liu Wen-Peng(刘文鹏)[a)b)],
Yin Shao-Tang(殷绍唐)[a)b)], and Jiang Hai-He(江海河)[c)]

[a)] *Crystal Lab, Anhui Institute of Optics and Fine Mechanics, Chinese Academy of Sciences, Hefei* 230031, *China*

[b)] *Anhui Provincial Key Lab of Optical Devices and Materials, Anhui Institute of Optics and Fine Mechanics, Chinese Academy of Sciences, Hefei* 230031, *China*

[c)] *Hefei Institutes of Physical Science, Chinese Academy of Sciences, Hefei* 230031, *China*

(Received 27 October 2009; revised manuscript received 8 December 2009)

A method to compute the numerical derivative of eigenvalues of parameterized crystal field Hamiltonian matrix is given, based on the numerical derivatives the general iteration methods such as Levenberg–Marquardt, Newton method, and so on, can be used to solve crystal field parameters by fitting to experimental energy levels. With the numerical eigenvalue derivative, a detailed iteration algorithm to compute crystal field parameters by fitting experimental energy levels has also been described. This method is used to compute the crystal parameters of Yb^{3+} in Sc_2O_3 crystal, which is prepared by a co-precipitation method and whose structure was refined by Rietveld method. By fitting on the parameters of a simple overlap model of crystal field, the results show that the new method can fit the crystal field energy splitting with fast convergence and good stability.

Keywords: crystal field parameter, numerical derivative of matrix eigenvalue, Yb^{3+}:Sc_2O_3, simple overlap model

PACC: 7510D, 7170C, 7170, 7800, 6100

1. Introduction

Fitting crystal parameters to a set of energy levels is the most frequently encountered problem in the crystal field theory,[1−9] which usually includes the following steps:[10]

(i) Estimate initial parameter values.

(ii) Construct energy matrix with initial parameter values.

(iii) Compute the matrix eigenvalues to obtain energy levels

(iv) Set up one-to-one correspondences between the experimental and calculated energy levels.

(v) Keep the eigenvectors of energy matrix fixed, determine the parameters by minimizing the sum of squares of the difference between the calculated and experimental energy levels.

(vi) Use the parameters obtained by step (v), return to step (ii) and continuously repeat steps (ii)–(v) until the calculated and experimental energy levels are judged to be in good enough agreement.

The process to minimize the sum of squares of the difference between the calculated and experimental energy levels in step (v) corresponds to solve the linear normal equation. This is one of its merits due to easiness to solve linear equation systems, and many sophisticated algorithms such as Gauss–Jordan method are available to do this.

Although the above method to compute crystal field parameters has been used at all times, and it is successful to fit +100 energy levels in lanthanide ions with good fitting quality,[11] it can be seen that this fitting process is not a real numerical iteration. To some extent, it is a quasi-guess process. The main difficulty in using the general numerical iteration algorithm to compute crystal field parameters is from the absence of an explicit mathematical expression between eigenvalues of energy matrix and fitted parameters, which

*Project supported by the National Natural Science Foundation of China (Grant Nos. 50772112 and 50872135), the Natural Science Foundation of Anhui Province of China (Grant No. 08040106820), the Knowledge Innovation Program of the Chinese Academy of Sciences (Grant No. YYYJ-1002).

†Corresponding author. E-mail: zql@aiofm.ac.cn

© 2010 Chinese Physical Society and IOP Publishing Ltd

results in the difficulty to compute the derivative of an eigenvalue of energy matrix with respect to fitted parameters, which is indispensible to obtain an iteration formula. In order to solve the difficulty, this paper will give a method to compute the eigenvalue derivative with respect to crystal field parameters, based on the derivative, the fitting process of crystal field parameters to split energy levels can be performed by the general numerical iteration methods such as the Leverberg–Marquardt method, Newton method, and so on. Meanwhile, a modified Levenberg–Marquardt algorithm with wide convergence range, high stability and fast convergence speed was given to fit crystal field parameters.

Rare earth sesquioxides with high thermal conductivity are promising hosts for high power solid state lasers pumped by laser diode, in particular scandium sesquioxide is a very promising laser medium for ultra-short pulse laser, which presents very interesting laser properties when it is doped moderately with Yb^{3+}.[12] Lupei *et al.*[13] and Elisabeth *et al.*[14] have reported the crystal energy splitting of Yb^{3+} at site C_2 and S_6 of Sc_2O_3 with space group $Ia3$. Merkle *et al.*[15] reported its temperature-depedent spectral and laser properties recently. There is no report on the crystal field parameter determination of Yb^{3+} in Sc_2O_3 to our knowledge.

The number of emission or absorption lines is very fewer than that of the crystal field parameters when Yb^{3+} is at the site of a low symmetry. For example, the independent crystal parameter number at C_2 symmetry is 15, at S_6 symmetry is 9, which is more than the number of absorption lines from the pure electronic states of Yb^{3+}:Sc_2O_3 at low temperature. Simple overlap model (SOM), proposed by Malta[16,17] and based on the crystal structural data, only uses 2∼3 parameters to describe crystal field interaction on magnetic ion, which can give a satisfactory fitting consistence between the experimental and calculated crystal field energy splitting[18−20] in many cases. So it is a suitable way to use SOM to obtain crystal field parameters and wave functions of Yb^{3+} in Sc_2O_3, by which it is possible to compute further spectral properties such as transition intensity.

In this paper, polycrystalline (5 at%) Yb^{3+}:Sc_2O_3 was prepared by a co-precipitation method, which can decrease sintering temperature obviously by about 200 °C to obtain pure cubic phase Yb^{3+}:Sc_2O_3, and its structure was determined by Rietveld method with x-ray powder diffraction, which would provide the structure parameters needed by SOM computation. Then the SOM parameters of Yb^{3+}:Sc_2O_3 were determined by the above iteration method, by which the crystal field parameters and wavefunctions of Yb^{3+} in Sc_2O_3 were computed. Fitting results show that it is a viable way by an iteration method to solve crystal field parameters using the eigenvalue numerical derivatives given here.

2. Method for fitting crystal field parameters

The Hamiltonian of a magnetic ion in crystal field can be expressed by the sum as follows:

$$H = \sum_{i=1}^{M} H_i = \sum_{i=1}^{M} P_i O_i, \tag{1}$$

where P_i is a parameterized value, which usually is determined by fitting experimental energy levels, O_i is operator on single electron, whose matrix elements usually can be computed directly. In order to obtain eigenvalues and eigenvectors, the matrix elements of O_i in the linear space spanned by bases $\{\psi_1, \psi_2, \ldots, \psi_N\}$ should be computed by

$$\boldsymbol{O}^i_{lm} = \langle \psi_l | O_i | \psi_m \rangle. \tag{2}$$

Matrix of the Hamiltonian correspondingly is expressed as

$$\boldsymbol{H} = \sum_{i=1}^{M} \boldsymbol{H}_i = \sum_{i=1}^{M} P_i \boldsymbol{O}^i, \tag{3}$$

where the element of row l and column m of matrix O^i is $\boldsymbol{O}^i_{lm}$.

The eigenvalue equation can be expressed as

$$\boldsymbol{H}\boldsymbol{\Psi} = \sum_{i=1}^{M} P_i \boldsymbol{O}^i \boldsymbol{\Psi} = E\boldsymbol{\Psi}, \tag{4}$$

where $\boldsymbol{\Psi}$ is eigenvector.

If a series of experimental energy levels $E_j^{\exp}(j = 1, \ldots, N)$ have been obtained, these values would be used to fit Hamiltonian parameter P_i $(i = 1, \ldots, M)$. The fitting procedure means that the following equation will take the minimum

$$\phi(\boldsymbol{P}) = \frac{1}{2}\boldsymbol{f}^{\mathrm{T}}\boldsymbol{f} = \frac{1}{2}\sum_{j=1}^{N} (E_j^{\exp} - E_j(\boldsymbol{P}))^2, \tag{5}$$

where $\boldsymbol{f}^{\mathrm{T}} = (E_1^{\exp} - E_1(\boldsymbol{P}), E_2^{\exp} - E_2(\boldsymbol{P}), \ldots, E_N^{\exp} - E_N(\boldsymbol{P}))$, $\boldsymbol{P}^{\mathrm{T}} = (P_1, P_2, \ldots, P_M)$, T stands for the

transpose operation on matrix, and E_j is the j-th eigenvalue computed from Eq. (4). Equation (5) is the implicit function of $\boldsymbol{P}$, which has no explicit mathematical relation between $\boldsymbol{P}$ and φ, which results in the difficulty to solve $\boldsymbol{P}$.

The extremal condition of Eq. (5) with variable $\boldsymbol{P}$, namely normal equation, is

$$g(\boldsymbol{P}) = \nabla\phi(\boldsymbol{P}) = D\boldsymbol{f}^{\mathrm{T}}\boldsymbol{f} = 0, \tag{6}$$

where,

$$D\boldsymbol{f}(\boldsymbol{x})^{\mathrm{T}} = \begin{bmatrix} \dfrac{\partial f_1}{\partial P_1} & \cdots & \dfrac{\partial f_2}{\partial P_1} & \cdots & \dfrac{\partial f_N}{\partial P_1} \\ \vdots & & \vdots & & \vdots \\ \dfrac{\partial f_1}{\partial P_M} & \cdots & \dfrac{\partial f_2}{\partial P_M} & \cdots & \dfrac{\partial f_N}{\partial P_M} \end{bmatrix}. \tag{7}$$

In order to construct iteration solution formula of Eq. (6), it is necessary to obtain the value of $\partial f_j/\partial P_i$ $(i = 1, \ldots, M, j = 1, \ldots, N)$. If these values can be obtained, general iteration methods such as Newton method, bisection method can be used to solve the parameter $\boldsymbol{P}$. As mentioned above, there is no explicit expression equation between $\boldsymbol{f}$ and $\boldsymbol{P}$, so it is impossible to get an analytical explicit equation of $\partial f_j/\partial P_i$ $(i = 1, \ldots, M, j = 1, ..., N)$. Now we seek numerical method to conquer this difficulty.

Let a parameter P_i varies as $P_i - \varepsilon$ and $P_i + \varepsilon$, where ε is a very small quantity, which results in the variation of eigenvalues $\boldsymbol{E}$ ($\boldsymbol{E}^{\mathrm{T}} = (E_1, E_2, \ldots, E_N)$) of Eq. (4) as $\boldsymbol{E}'$ and $\boldsymbol{E}''$, respectively, and the corresponding characteristic equation variation of $\boldsymbol{H}$ matrix is

$$\begin{vmatrix} (P_i+\varepsilon)O^i_{11} - E'' & (P_i+\varepsilon)O^i_{12} \ldots (P_i+\varepsilon)O^i_{1N} \\ (P_i+\varepsilon)O^i_{21} & (P_i+\varepsilon)O^i_{12} - E'' \ldots (P_i+\varepsilon)O^i_{2N} \\ \vdots & \vdots \\ (P_i+\varepsilon)O^i_{N1} & (P_i+\varepsilon)O^i_{N2} \ldots (P_i+\varepsilon)O^i_{NN} - E'' \end{vmatrix} - \begin{vmatrix} (P_i-\varepsilon)O^i_{11} - E' & (P_i-\varepsilon)O^i_{12} \ldots (P_i-\varepsilon)O^i_{1N} \\ (P_i-\varepsilon)O^i_{21} & (P_i-\varepsilon)O^i_{12} - E' \ldots (P_i-\varepsilon)O^i_{2N} \\ \vdots & \vdots \\ (P_i-\varepsilon)O^i_{N1} & (P_i-\varepsilon)O^i_{N2} \ldots (P_i-\varepsilon)O^i_{NN} - E' \end{vmatrix}$$

$$= \begin{vmatrix} 2\varepsilon O^i_{11} - (E'' - E') & 2\varepsilon O^i_{12} \ldots 2\varepsilon O^i_{1N} \\ 2\varepsilon O^i_{21} & 2\varepsilon O^i_{12} - (E'' - E') \ldots 2\varepsilon O^i_{2N} \\ \vdots & \vdots \\ 2\varepsilon O^i_{N1} & 2\varepsilon O^i_{N2} \ldots 2\varepsilon O^i_{NN} - (E'' - E') \end{vmatrix},$$

which corresponds to the eigenvalue equation:

$$2\varepsilon\boldsymbol{O}^i\Psi = (E'' - E')\boldsymbol{O}^i\Psi = \Delta E\Psi, \tag{8}$$

where $\Delta E = E'' - E'$.

According to Eq. (8), the derivative of $\boldsymbol{E}$ can be defined as

$$\frac{\partial \boldsymbol{E}}{\partial P_i} = \lim_{\delta\to 0}\frac{D(2\varepsilon\boldsymbol{O}^i)}{2\varepsilon} = \lim_{\Delta\to 0}\frac{D(\Delta\boldsymbol{O}^i)}{\Delta}, \tag{9}$$

where $\Delta = 2\varepsilon$, $\Delta\boldsymbol{O}^i = 2\varepsilon \mathrm{O}^i$, which stands for matrix variation of Hamiltonian caused by variation 2ε of parameter P_i, D stands for the operation to solve eigenvalues of matrix $\Delta\boldsymbol{O}^i$ by diagonalizing it, $\boldsymbol{E}^{\mathrm{T}} = (E_1, \ldots, E_N)$. Now it is easy to compute numerical derivative of eigenvalues with small variable Δ by

$$\frac{\partial \boldsymbol{E}}{\partial P_i} \approx \frac{D(\Delta\boldsymbol{O}^i)}{\Delta}. \tag{10}$$

So the derivative of $\partial f_j/\partial P_i$ can be expressed as

$$\frac{\partial f_j}{\partial P_i} = -\frac{\partial E_j}{\partial P_i} \approx -\frac{D(\Delta\boldsymbol{O}^i)_j}{\Delta}, \tag{11}$$

where $D(\Delta\boldsymbol{O}^i)_j$ represents the j-th eigenvalue obtained by diagonalizing matrix $\Delta\boldsymbol{O}^i$. Especially, if $\boldsymbol{O}^i$ is diagonal, the following result can be obtained immediately:

$$\frac{\partial f_j}{\partial P_i} = -\frac{D(\Delta\boldsymbol{O}^i)_j}{\Delta} = \frac{\Delta\boldsymbol{O}^i_{jj}}{\Delta} = \boldsymbol{O}^i_{jj}. \tag{12}$$

After the derivative of energy $\boldsymbol{E}$ is obtained, the iteration method can be used to solve Hamiltonian parameter $\boldsymbol{P}$. Levenbery–Marquardt iteration method with good stability, large convergence region and fast convergence speed, is a very excellent algorithm and can be used to solve P, whose iteration formulas[21] are

$$\boldsymbol{x}^{k+1} = \boldsymbol{x}^k - [\hat{\boldsymbol{G}}(\boldsymbol{x}^k)]^{-1}\boldsymbol{D}\boldsymbol{f}(\boldsymbol{x}^k)^{\mathrm{T}}\boldsymbol{f}(\boldsymbol{x}^k), \tag{13}$$

$$\hat{\boldsymbol{G}}(\boldsymbol{x}^k) = \boldsymbol{D}\boldsymbol{f}(\boldsymbol{x}^k)^{\mathrm{T}}\boldsymbol{D}\boldsymbol{f}(\boldsymbol{x}^k) + \mu_k \boldsymbol{I}, \tag{14}$$

where $\boldsymbol{x} = \boldsymbol{P}$, μ_k is damping factor, which can be adjusted during iteration, $\boldsymbol{I}$ is unit matrix. Based on the algorithm of Li *et al.*,[21] a modified iteration method is described as follows:

Step 1 The initial parameter values of P are assigned to $\boldsymbol{x}^0$ and $\boldsymbol{x}^1$, iteration precision, initial damping factor, scaling constant (> 1) of the damping factor, maximal loop number to search the damping factor, maximal iteration loop number are assigned to ε, μ, ν, CLAMax, and CLBMax, respectively. Iteration count variable CLB are assigned by 1.

Step 2 CLA $\leftarrow$ 1, $\boldsymbol{x}^0 \leftarrow \boldsymbol{x}^1$, and to compute $\boldsymbol{f}(\boldsymbol{x}^0)$, $\boldsymbol{D}\boldsymbol{f}(\boldsymbol{x}^0)$, $\boldsymbol{D}\boldsymbol{f}(\boldsymbol{x}^0)^{\mathrm{T}}\boldsymbol{f}(\boldsymbol{x}^0)$, $\boldsymbol{D}\boldsymbol{f}(\boldsymbol{x}^0)^{\mathrm{T}}\boldsymbol{D}\boldsymbol{f}(\boldsymbol{x}^0)$, and $\boldsymbol{\phi}(x^0)$.

Step 3 To compute

$$\begin{aligned}\Delta\boldsymbol{x}^0 = &-[\boldsymbol{D}\boldsymbol{f}(\boldsymbol{x}^0)^{\mathrm{T}}\boldsymbol{D}\boldsymbol{f}(\boldsymbol{x}^0) + \mu_0\boldsymbol{I}]^{-1} \\ &\times [\boldsymbol{D}\boldsymbol{f}(\boldsymbol{x}^0)^{\mathrm{T}}\boldsymbol{f}(\boldsymbol{x}^0)],\end{aligned}$$

$\boldsymbol{x}^1 = \boldsymbol{x}^0 + \Delta\boldsymbol{x}^0$, and $\phi(\boldsymbol{x}^1)$.

Step 4 If $\phi(\boldsymbol{x}^1) \geq \phi(\boldsymbol{x}^0)$ then

(a) If CLA = CLAMax, go to Step 5.

(b) If CLA $<$ CLAMax, then CLA $\leftarrow$ CLA + 1, $\mu \leftarrow \mu\nu$, and go to Step 3.

If $\phi(\boldsymbol{x}^1) < \phi(\boldsymbol{x}^0)$, go to Step 5.

Step 5 $\mu \leftarrow \mu/\nu$, and to compute

$$\begin{aligned}\Delta x^1 = &-[\boldsymbol{D}\boldsymbol{f}(\boldsymbol{x}^0)^{\mathrm{T}}\boldsymbol{D}\boldsymbol{f}(\boldsymbol{x}^0) + \mu_0\boldsymbol{I}]^{-1} \\ &\times [\boldsymbol{D}\boldsymbol{f}(\boldsymbol{x}^0)\boldsymbol{f}(\boldsymbol{x}^0)],\end{aligned}$$

$\boldsymbol{x}^2 = \boldsymbol{x}^0 + \Delta\boldsymbol{x}^1$ and $\phi(\boldsymbol{x}^2)$.

Step 6 If $\phi(\boldsymbol{x}^2) < \phi(\boldsymbol{x}^1)$, then $\boldsymbol{x}^1 \leftarrow \boldsymbol{x}^2$, $\phi(\boldsymbol{x}^1) \leftarrow \phi(\boldsymbol{x}^2)$, and go to Step 7, otherwise go to Step 7 directly.

Step 7 If

$$||\Delta\boldsymbol{x}^1|| < \varepsilon$$

or

$$||\boldsymbol{D}\boldsymbol{f}(\boldsymbol{x}^0)^{\mathrm{T}}\boldsymbol{f}(\boldsymbol{x}^0)|| < \varepsilon,$$

then it is thought that precision is reached, to save iteration information, and exit iteration, otherwise to do the following:

If CLB $<$ CLBMax, then CLB $\leftarrow$ CLB + 1, go to Step 2.

If CLB = CLBMax, to save information and exit iteration.

It can be seen that a numerical iteration to solve crystal parameter is realized after the numerical derivative of eigenvalues with respect to Hamiltonian parameter is found.

3. Crystal field energy fitting of Yb^{3+}:Sc_2O_3

3.1. Preparation and structure of Yb^{3+}:Sc_2O_3

3.1.1. Preparation of Yb^{3+}:Sc_2O_3

The 5-at% Yb^{3+}:Sc_2O_3 was prepared by co-precipitation technique using ammonia as precipitant. Aqueous nitrate solutions of rare earth oxide were prepared by dissolving Yb_2O_3 and Sc_2O_3 with purity 99.999% into an excess amount of nitric acid, respectively, which is stirred and heated at 80–90 °C during dissolving Y_2O_3 and Sc_2O_3. And then the nitrate solutions of Yb_2O_3 and Sc_2O_3 were mixed together by a molar ratio of Yb^{3+}:Sc^{3+} = 0.05:0.95. The mixed nitrate solution (concentration of Yb^{3+} being 0.0125 M, concentration of Sc^{3+} being 0.2375 M) was added dropwise into ammonia water (concentration of OH^- being 1.5 M) under mild stirring at room temperature. After the titration, the PH value of suspension was kept 8–9. After precipitation was over, the precipitate slurry was washed with deionized water by a centrifugal machine for four times. Then the precipitate was dried in electronic oven at 90 °C for 12 h, and the obtained precursor was ground into powder and calcined at 1000 °C for 2 h in air atmosphere. After the sample is cool down to room temperature, it was ground into powder and was used as the sample of x-ray diffraction (XRD).

3.1.2. Structure determination of Yb^{3+}:Sc_2O_3

The powder XRD was carried out by using a Philips X'pert PRO diffractometer with Cu Kα radiation at room temperature in step scan mode in the range of 20° to 80° with step interval 0.03°. Through XRD pattern the structure of Yb^{3+}:Sc_2O_3 was refined by general structure analysis system (GSAS)[22] using a full-profile fitting method, namely Rietveld method. Using the structure data of Sc_2O_3 [JCPDS-ICCD database, card No. 43-1028] as initial values of refinement and pseudo-Voigt profile, we refine thirty-eight parameters including atom coordinates, temperature factors, profile parameters, background curve parameters, and so on, the refined results are shown in Fig. 1 and Table 1. It can be seen that the observed

and calculated XRD patterns are consistent very well, which is also shown by the small residuals $R_{\rm p} = 3.5\%$, $R_{\rm wp} = 4.7\%$, and $R(F^2) = 0.023$. The value of $D_{\rm dw}$, a statistical measure of the serial correlation in the powder pattern differences, is 1.428. If no serial correlation is presented in the differences then $D_{\rm dw}$ is close to 2. The value of $D_{\rm dw}$ indicates that profile model is good and a systematic error is small. On the other hand, experience has shown that the principal systematic errors in most Rietveld refinements are in the profile functions and that they have little effect on the structural parameters resulting from the least squares analysis. So we can conclude that the good structure parameters of 5-at% Yb:Sc_2O_3 are obtained here.

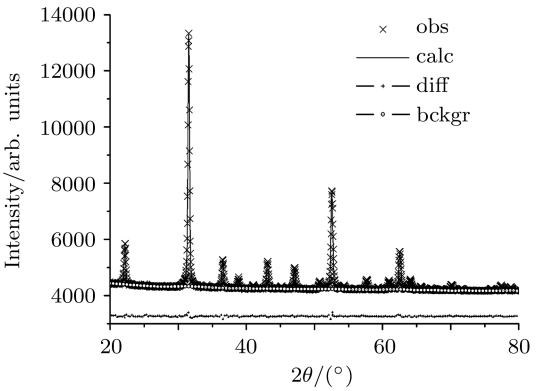


Fig. 1. The observed (obs), calculated (calc), background (bckgr) and difference (diff) powder XRD patterns of 5-at% Yb^{3+}:Sc_2O_3 at room temperature.

Table 1. Structural parameters of 5-at% Yb^{3+}:Sc_2O_3, whose space is $Ia3$ and refined lattice parameter a = 9.883905(53) Å (1 Å = 0.1 nm).

atom	Wyckoff site	x, y, z	$U_{\rm iso}$
Sc/Yb	8b	0.2500, 0.2500, 0.2500	0.05807
Sc/Yb	24d	–0.0348, 0.0000, 0.2500	0.06039
O	48 e	0.3909, 0.1545, 0.3813	0.04786

The site symmetry of Yb^{3+} at 24d and 8b of $Ia3$ are C_2 and S_6, whose two-fold and three-fold symmetry axes are along the direction of [100] and [111]. During our crystal field parameter computation, the principal axis is the direction [001]. So the coordinates $\boldsymbol{X}$ of ligands of Yb^{3+} in the above crystallography coordinates should be transformed by

$$\boldsymbol{X}' = \boldsymbol{A}\boldsymbol{X},$$

where

$$\boldsymbol{X}^{\rm T} = (x, y, z),$$
$$\boldsymbol{X}'^{\rm T} = (x', y', z'),$$

the principal of $\boldsymbol{X}'$ of 24d and 8b are along the direction [001]. The transform matrices $\boldsymbol{A}$ are $\begin{bmatrix} 0 & 0 & -1 \\ 0 & 1 & 0 \\ 1 & 0 & 0 \end{bmatrix}$ and $\begin{bmatrix} 1/\sqrt{6} & 1/\sqrt{6} & -2/\sqrt{6} \\ -1/\sqrt{2} & 1/\sqrt{2} & 0 \\ 1/\sqrt{3} & 1/\sqrt{3} & 1/\sqrt{3} \end{bmatrix}$, respectively.

3.2. Energy fitting of Yb^{3+}:Sc_2O_3

3.2.1. Simple overlap model (SOM) of crystal field

The SOM is based on the following assumption: i) potential energy $V_{\rm CF}$ of nl electrons from the first neighbours is equivalent to that created by charges uniformly distributed in small regions around the middle of the central ion-ligand distance; ii) the total charge from the μ-th ligand region is $g_\mu \rho_\mu e$, where g_μ is a charge factor, ρ_μ is the overlap between the central ion and the μ-th ligand, e is unit charge. The overlap depends on the ligand type and the distance between central ion and ligand, which can be assumed to be a function of the shortest central ion-ligand distance r_0 as

$$\rho_\mu = \rho_0 \left(\frac{r_0}{r_\mu}\right)^n, \tag{15}$$

where n is taken as 3.5 generally. Finally $V_{\rm CF}$ is expressed as

$$V_{\rm CF} = \sum_{kq} B_q^k C_q^k, \tag{16}$$

where

$$B_q^k = \sum_\mu g_\mu \rho_\mu (2\beta_\mu)^{k+1} {\rm Y}_q^{k*}(\boldsymbol{r}_\mu)', \tag{17}$$

$${\rm Y}_q^{k*}(\boldsymbol{r}_\mu)' = -e^2 \langle r^k \rangle \sqrt{\frac{4\pi}{2k+1}} \frac{{\rm Y}_q^{k*}(\boldsymbol{r}_\mu)}{r_\mu^{k+1}}, \tag{18}$$

in which $Y_q^{k*}(\boldsymbol{r}_\mu)$ is spherical harmonics, $*$ stands for the complex conjugate operation, $\boldsymbol{r}_\mu$ is the position vector originated from central-ion of the μ-th ligand, $\langle r^k \rangle$ is radial integrals which are given by Ref. [23],

$$\beta_\mu = \frac{1}{1 \pm \rho_\mu}. \tag{19}$$

As far as Yb^{3+} in Sc_2O_3, the plus sign is taken in Eq. (19).

3.2.2. Energy fitting details of Yb^{3+} in Sc_2O_3

(I) Matrix elements evaluation

As far as Yb^{3+} in Sc_2O_3, its configuration is $4f^{13}$, which has two multiplets $^2F_{7/2}$ and $^2F_{5/2}$. The two multiplets with the different J values were split by spin–orbital interaction

$$H_{sl} = \sum_i \xi_{nl} \boldsymbol{s}_i \cdot \boldsymbol{l}_i. \tag{20}$$

According to Refs. [24] and [25], the matrix elements of H_{sl} in linear space $\{|f^{13}SLJM\rangle\}$ can be evaluated as

$$\langle f^{13}SLJM|H_{sl}|f^{13}S'L'J'M'\rangle = -\xi_{nl}\delta_{SS'}\delta_{LL'}\delta_{JJ'}\delta_{MM'}(-1)^{S'+L+J}\begin{Bmatrix} S' & L' & J \\ L & S & 1 \end{Bmatrix}\sqrt{126}. \tag{21}$$

The crystal field interaction $V_{\rm CF}$ on Yb^{3+} results in the further splitting of multiplets $^{2S+l}L_J$, whose angular part of matrix elements can be evaluated as[3,4]

$$\begin{aligned} &\langle 4f^{13}SLJM|C_q^k|4f^{13}S'L'J'M'\rangle \\ &= (-1)^{J-M}\begin{pmatrix} J & k & J' \\ -M & q & M' \end{pmatrix} \times \langle 4f^{13}SLJM||U^{(k)}||f^{13}S'L'J'M'\rangle\langle f||c^{(k)}||f\rangle, \end{aligned} \tag{22}$$

$$\begin{aligned} &\langle 4f^{13}SLJM||U^{(k)}||f^{13}S'L'J'M'\rangle \\ &= (-1)^{S+L'+J+2k}([J][J'])^{1/2}\begin{Bmatrix} J & J' & k \\ L' & L & S \end{Bmatrix} \times \langle 4f^1SL||U^{(k)}||f^1S'L'\rangle. \end{aligned} \tag{23}$$

Summarily, the spin–orbital and crystal field should be included when we fit crystal field energy levels of Yb^{3+}:Sc_2O_3.

(II) Parameter fitting to energy levels of Yb^{3+}:Sc_2O_3

According to the previous discussion, it is very easy to compute the numerical derivative of eigenvalues with respect to the variable spin–orbital parameter ξ. It is not the case to compute that with respect to the charge factor g_μ and overlap parameter ρ_0. If these variables change by Δ, this will result in the variation δB_q^k of B_q^k, which can be evaluated approximately as

$$(\delta B_q^k)_i \approx \frac{\partial B_q^k}{\partial x_i}\Delta, \tag{24}$$

where $x_1 = g_\mu, x_2 = \rho_0$.

From Eqs. (17)–(19), it is easy to obtain the following equations:

$$\frac{\partial B_q^k}{\partial g_\mu} = \sum_\mu \rho_\mu (2\beta_\mu)^{k+1} \mathrm{Y}_q^{k*}(\boldsymbol{r}_\mu)', \tag{25}$$

$$\begin{aligned} \frac{\partial B_q^k}{\partial \rho_0} &= \pm 2^{1+k}(1+k)\sum_\mu g_\mu \left(\frac{r_0}{r_\mu}\right)^n \\ &\quad \times \rho_\mu \left(\frac{1}{1\mp\rho_\mu}\right)^{k+2} \mathrm{Y}_q^{k*}(\boldsymbol{r}_\mu)'. \end{aligned} \tag{26}$$

Then the numerical derivatives of eigenvalues with respect to g_μ and ρ_μ are given by

$$\frac{\partial E_j}{\partial x_i} \approx \frac{D((\delta B_q^k)_i \boldsymbol{C}_k^q)_j}{\Delta}, \tag{27}$$

where $\boldsymbol{C}_k^q$ represents the matrix of C_k^q. Thus, all the values needed in iteration Eqs. (13) and (14) to solve g, ρ_0 and ξ by fitting energy levels of Yb^{3+}:Sc_2O_3 have been gotten. The fitting consistence can be indicated by residual R and root-mean-square deviation σ, which are defined as

$$R = \sqrt{\sum_i \left(E_i - E_i^{\rm cal}\right)^2 / \sum_i E_i^2}, \tag{28}$$

$$\sigma = \sqrt{\sum_i \left(E_i - E_i^{\rm cal}\right)^2 / (N-M)}. \tag{29}$$

Using the initial values $(g_j, \rho_0) = (-0.85, 0.20)$, scaling factor $\nu = 5$, initial damping factor $\mu = 0.1$, CLAMax = 60, CLBMax = 10, $\xi = 2900\ \mathrm{cm}^{-1}$, we fit the parameters of SOM, the fitting results are shown in Table 2. The residuals R for Yb^{3+} at site 24d and 8b are 0.66% and 0.81%, which are very small and indicate that the fitting effect is very good.

If g_j, ρ_0, and ξ are fitted synchronously, poor initial value of ξ would affect the iteration results of g_j and ρ_0 seriously. For example, for Yb^{3+} of 24d, initial values (g_j, ρ_0, ξ) = (−0.85, 0.20, 2800) would give fitting results (g_j, ρ_0, ξ) = (−1.25, 0.176, 2804.70) and R = 2.5%, which indicate that this is a poor fitting. Initial values (g_j, ρ_0, ξ) = (−0.85, 0.20, 2900) would give fitting results (g_j, ρ_0, ξ) = (−1.06, 0.297, 2900.44) and R = 0.67%, which indicate that this is a good fitting. It is obvious that variation of ξ can affect the values of g_j and ρ_0. So it is important to provide good initial value of ξ, which would be helpful for decreasing parameter interaction. It has similar effect on g_j and ρ_0 to add another parameter n in Eq. (15) as fitted variable.

Table 2. Energy levels of Yb^{3+}:Sc_2O_3, whose fitting initial values and results.

	24d (C_2)		8b (S_6)	
g_j	–1.06		–0.72	
ρ_0	0.296		0.14	
ξ/cm^{-1}	2900		2900	
observed levels E/cm^{-1}	0, 580, 650, 1110		0, 323, 50, 900	
	10258, 10620, 11190		10260, 10505, 11010	
calculated levels	0, 544, 582, 1109		0, 261, 635, 844,	
E^{cal}/cm^{-1}	10281, 10712, 11172		10227, 10580, 10974	
B_q^k	k, q		k, q	
	2, 2	–301.6+865.1I	2, 0	–1185.1
	2, 0	–255.5	4, 3	–1109.0+119.8I
	4, 4	916.4+218.7I	4, 0	–577.0
	4, 2	–21.8+1103.5	6, 6	346.8–75.8I
	4, 0	–947.8	6, 3	173.1–18.7I
	6, 6	68.3+71.9I	6, 0	533.2
	6, 4	–561.7+24.4I		
	6, 2	–24.2+9.6I		
	6, 0	156.4		
R(%)	0.66		0.81	
σ/cm^{-1}	48		65	
CLA	20		60	
CLB	8		5	
μ	9.3×10^{19}		22334	

It should be pointed out that there is also interaction between parameters g_j and ρ_0, which can be seen from Eqs. (15), (17) and (19). Different initial values of g_j and ρ_0 may result in the different fitting values of them. For example, for Yb^{3+} of 24d with C_2 site symmetry, if (g_j, ρ_0) = (−0.85, 0.05) was used as the iteration initial values, final iteration values (g_j, ρ_0) = (−2.059, 0.0719) would be obtained with R = 0.78%, CLA = 26, CLB = 4, $\mu = 4.7\times10^{20}$, and calculated energy levels 0, 565, 662, 1111, 10331, 10743, 11186 cm^{-1}. It can be seen that energy fitting for $^2F_{7/2}$ splitting is very good, and the differences between calculated and observed values are 0, 15, −12 and −1 cm^{-1}, respectively. For the energy fitting of $^2F_{5/2}$ splitting, differences are −73, −123, and −4 cm^{-1}, which have larger differences between observed and calculated values. Compared this fitting result with the previous fitting result, we can find that the absolute value of g_j increases and ρ_0 decreases, which reflects the interaction of g_j and ρ_0.

Crystal field causes the J-mixing and M-mixing of Yb^{3+} in Sc_2O_3. Due to large energy gap between $^2F_{7/2}$ and $^2F_{5/2}$, J-mixing is not serious and can be omitted. For wavefunctions of 0, 580, 650, 1110 cm^{-1} of Yb^{3+} at site 24d, their component ratio with $J = 7/2$ is more than 99%, and for the wavefunctions of 10258, 10620, 11190 cm^{-1} of Yb^{3+} at site 24d, their component ratio with $J = 5/2$ is more than 99%. It is very similar to this for the wavefunctions of Yb^{3+} at site 8b with symmetry S_6. M-mixing is so serious that wavefunctions cannot be named by a leading component $|SLJM\rangle$. For example, the wavefunction component ratios of Yb^{3+} at site 24 corresponding to $E = 0$ and 650 cm^{-1} are

$E = 0$ cm^{-1}:

$\Psi_1 : (38.75\%)|^2F, 7/2, -5/2\rangle + (35.2\%)|^2F, 7/2, 3/2\rangle + (25.8\%)|^2F, 7/2, -1/2\rangle + (0.15\%)|^2F, 7/2, 7/2\rangle,$
$\Psi_2 : (38.75\%)|^2F, 7/2, 5/2\rangle + (35.2\%)|^2F, 7/2, -3/2\rangle + (25.8\%)|^2F, 7/2, 1/2\rangle + (0.15\%)|^2F, 7/2, -7/2\rangle,$
$E = 650\ \mathrm{cm}^{-1}$:
$\Psi_5 : (48.65\%)|^2F, 7/2, -5/2\rangle + (19.8\%)|^2F, 7/2, 3/2\rangle + (19.3\%)|^2F, 7/2, 7/2\rangle + (12.2\%)|^2F, 7/2, -1/2\rangle,$
$\Psi_6 : (48.65\%)|^2F, 7/2, 5/2\rangle + (19.8\%)|^2F, 7/2, -3/2\rangle + (19.3\%)|^2F, 7/2, -7/2\rangle + (12.2\%)|^2F, 7/2, 1/2\rangle.$

It can be seen that the leading components of Ψ_1 and Ψ_5 are the same, and that of Ψ_2 and Ψ_6 are the same. Whereas Ψ_1 and Ψ_2, Ψ_5 and Ψ_6 are degenerated due to time inversion symmetry, and in the degenerated wavefunctions, components of $|SLJM\rangle$ and $|SLJ - M\rangle$ have the same ratio.

4. Conclusion

This paper gives a method to compute the numerical derivative of eigenvalues of the parameterized crystal field Hamiltonian matrix, using which we can construct a real iteration algorithm for fitting crystal field energy splitting. Based on the numerical derivatives, a modified Levenbergy–Marquardt iteration algorithm was given. At the same time, a polycrystalline (5 at%) Yb^{3+}:Sc_2O_3 was prepared by co-precipitation method, its structure was determined by XRD and refined by Rietveld method. Using the obtained structural parameters, the parameters of SOM were fitted to energy splitting of Yb^{3+}:Sc_2O_3 by the modified iteration algorithm, and the fitted energy levels were consistent with the experimental values very well. The fitting results indicate that the new method being a real iteration numerical method is a successful way to fitting crystal field parameters.

References

[1] Chi Y B, Liu S X, Li H N, Zhao X Y and Wang L Z 1997 *Chin. Phys.* **6** 429

[2] Yang Z Y and Hao Y 2005 *Acta Phys. Sin.* **54** 2883 (in Chinese)

[3] Wei Q, Yang Z Y, Wang C J and Xu Q M 2007 *Acta Phys. Sin.* **56** 507 (in Chinese)

[4] Xia S D, Huang F H and Xu P S 1984 *Acta Phys. Sin.* **33** 1160 (in Chinese)

[5] Chen X Y and Luo Z D 1999 *Chin. Phys.* **8** 607

[6] Du X B, Jin H M, Su G, Wang X Q, Xu S W and Yan Y 2005 *Chin. Phys.* **14** 2127

[7] Du X B, Jin H M, Ma R G, Su F, Wang X Q, Yan Y and Zhang Y X 2006 *Chin. Phys.* **15** 2146

[8] Han K, Ye S W and Yin C H 2003 *Acta Phys. Sin.* **52** 2280 (in Chinese)

[9] Jiao Y, Ru R P, Song N, Yang L, Yin C H, Zhang L and Zhao J P 2006 *Acta Phys. Sin.* **55** 6055 (in Chinese)

[10] Newman D J and Betty N G 2000 *Crystal Field Handbook* (Cambridge: Cambridge University Press) p. 43

[11] Newman D J and Betty N G 2000 *Crystal Field Handbook* (Cambridge: Cambridge University Press) p. 120

[12] Bravo A C, Longuet L, Autissier D, Baumard J F, Vissie P and Longuet J L 2009 *Opt. Mater.* **31** 734

[13] Lupei V, Lupei A and Ikesue A 2005 *Appl. Phys. Lett.* **86** 111118-1

[14] Antic-Fidancev E, Hölsá J and Lastusaari M 2003 *J. Phys.: Condens. Matter* **15** 863

[15] Merkle L D, Newburgh G A, Ter-Gabrielyan N, Michael A and Dubinskii M 2008 *Opt. Commun.* **281** 5855

[16] Malta O L 1982 *Chem. Phys. Lett.* **88** 353

[17] Malta O L 1982 *Chem. Phys. Lett.* **87** 27

[18] Gaume R, Viana B, Derouet J and Vivien D 2003 *Opt. Mater.* **222** 107

[19] Porcher P, Santos M C D and Malta O 1999 *Phys. Chem. Chem. Phys.* **1** 397

[20] Albuquerque R Q, Rocha G B, Malta O L and Porcher P 2000 *Chem. Phys. Lett.* **331** 519

[21] Li Q Y, Guan Z and Bai F S 2000 *Numerical Computation Principles* (Beijing: Tsinghua University Press) p. 294 (in Chinese)

[22] Larson A C and Von Dreele R B 2004 *General Structure Analysis System* (GSAS), Los Alamos National Laboratory Report LAUR 86-748

[23] Freeman A J and Desclaux J P 1979 *J. Magn. Mater.* **12** 11

[24] Xia S D 1994 *Group and Spectroscopy* (Beijing: Science Press) p. 176 (in Chinese)

[25] Nielson C W and Koster George F 1963 *Spectroscopic Coefficients for the p^n, d^n, and f^n Configurations* (Philadelphia: MIT Press) viii